Graphical Abstract

Leveraging Physics-Informed Neural Networks for Efficient Modelling of Coastal Ecosystems Dynamics: A Case Study of Sundarbans Mangrove Forest

Majdi Fanous, Alireza Daneshkhah, Jonathan M. Eden, Juntao Yang, Simon See, Vasile Palade

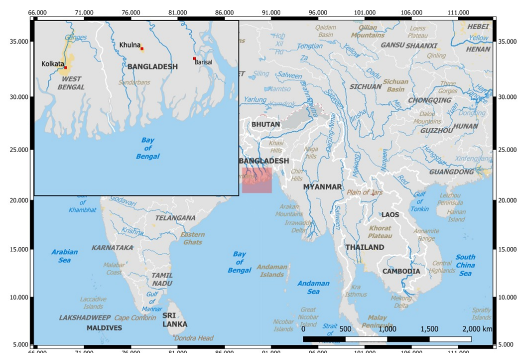

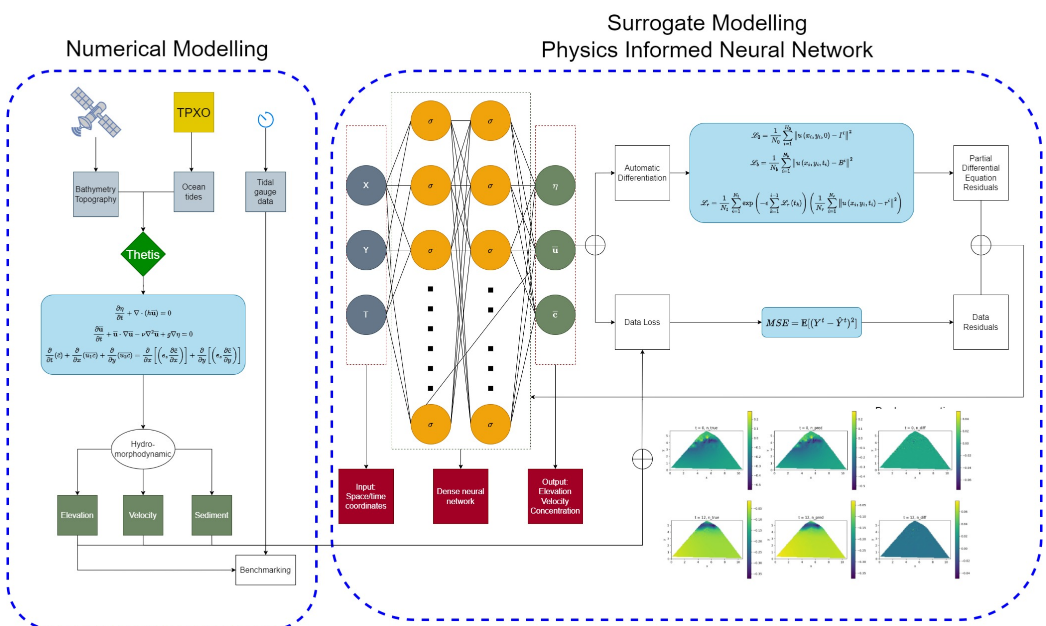

Highlights

Leveraging Physics-Informed Neural Networks for Efficient Modelling of Coastal Ecosystems Dynamics: A Case Study of Sundarbans Mangrove Forest

Majdi Fanous, Alireza Daneshkhah, Jonathan M. Eden, Juntao Yang, Simon See, Vasile Palade

- Introduces hybrid PINNs, merging physics-informed modeling and neural networks for advanced mangrove dynamics simulation.
- Utilises diverse datasets, including satellite imagery, simulations, and physics equations, ensuring comprehensive mangrove representation.
- Employs PINNs on complex PDE model, with complex boundary conditions and over an irregular and very large spatial domain.
- Significant time and computational improvements compared to traditional numerical model.

Leveraging Physics-Informed Neural Networks for Efficient Modelling of Coastal Ecosystems Dynamics: A Case Study of Sundarbans Mangrove Forest

Majdi Fanous[a,*], Alireza Daneshkhah[a], Jonathan M. Eden[b], Juntao Yang[c], Simon See[a,d], Vasile Palade[a]

[a] *Centre for Computational Science & Mathematical Modelling, Coventry University, Priory Street, Coventry, CV1 5FB, United Kingdom*
[b] *Centre for Agroecology, Water and Resilience, Coventry University, Ryton Gardens, Wolston Lane, Warwickshire, CV8 3LG, United Kingdom*
[c] *NVIDIA AI Technology Center, Temasek Blvd, Cityhall District, 038988, Singapore*
[d] *NVIDIA AI Technology Center, San Tomas Expy, Santa Clara, 95051, United States of America*

Abstract

Modelling mangrove environments is crucial for implementing effective protection measures and enhancing their resilience against climate change impacts, such as sea levels rise and land erosion. Traditionally, numerical modelling methods have been employed for this purpose; however, these methods are face time and computational complexities hindering the success of the protection and restoration projects. Recent advances in machine learning, particularly in physics-informed surrogate models, have gained attention for their ability to simulate complex dynamics while adhering to the governing physics equations. This paper introduces a novel hybrid physics-informed neural networks (PINNs) approach as a surrogate to the traditional and computationally expensive finite element (FE) numerical model. The proposed model is applied on complex boundary conditions and utilises heterogeneous data, including satellite imagery and simulations generated from numerical model as well as physics equations to constrain the solution of the output on a large and irregular spatial domain. To address the varying time dynamics across the large domain, a temporal causality weight is introduced to the loss function of the PINNs model, ensuring the minimisation of the loss on initial conditions before extending across the time domain. To demonstrate its effectiveness in modelling the complex and nonlinear interactions of mangrove ecosystems, the approach is applied to the Sundarbans, the world's largest

*Majdi Fanous
Email address: fanousm2@coventry.ac.uk (Majdi Fanous)

mangrove forest, situated in a climatically vulnerable region of South Asia. The study's findings revealed that PINNs significantly outperformed the numerical model exhibiting a five-fold decrease in computational cost, enabling near real-time predictions of mangrove dynamics. This improvement in computational efficiency is crucial for situations requiring rapid responses, such as evaluating the resilience of mangroves against extreme climate events like tropical cyclones. Furthermore, the accuracy of PINNs was found to be comparable, if not superior, to the traditional model enabling accurate capturing of the dynamics around the mangrove environments.

Keywords: Coastal erosion, Hybrid modelling, Hydro-morphodynamic modelling, Mangrove Environments, Physics-informed neural networks

---

1. Introduction

Considering the prevailing patterns of global warming, the projected escalation in sea levels entails the potential to trigger catastrophic consequences for coastal ecosystems, neighbouring communities, and interconnected marine ecosystems. Thus, developing proper climate mitigation and adaptation strategies is crucial for a better understanding of the resilience of such ecosystems against climate change impacts. One solution is the use of artificial barriers as defense against rising sea levels Losada et al. (2019), but this is often cost prohibitive. The United Nations, in its Intergovernmental Panel on Climate Change (IPCC) Sixth Assessment Report (AR6), therefore encouraged the use of natural defenses, known as ecosystem-based adaptation solutions, as an alternative to mitigate climate change impacts Cooley et al. (2022). Such defenses have huge potential to be an inexpensive, yet reliable, solution with the additional benefit of preserving natural ecosystems.

Among the most important natural defenses are mangrove ecosystems, which play a vital role in safeguarding coastal regions from the detrimental impacts of climate change, such as sea-level rise and land erosion Fanous et al. (2023b). Accurately modelling the complex dynamics of mangrove environments is crucial for implementing effective protection and restoration strategies. Traditionally, numerical modelling techniques such as finite difference, volume, or element methods have been employed for this purpose. However, these methods often face significant challenges related to time and computational complexities, which can hinder the success rates of proposed projects Fanous et al. (2023b). This is due to the fact that these models require high-resolution inputs, that account for spatial and temporal variations, to produce accurate solutions as well as solving complex physics equations, such as Navier–Stokes, that govern the hydro-morphodynamics of this region. Consequently, executing such models becomes time-consuming and impractical, especially when real-time or near real-time predictions are necessary for effective coastal adaptation decision-making.

An alternative approach to traditional numerical modelling is using machine learning models as surrogates, which can efficiently replace the existing solvers by learning the dynamics entirely from the data Pinto et al. (2021); Partee et al. (2022); Weber et al. (2020). The utilisation of progressively larger models and datasets in deep learning has resulted in significant advancements across various scientific disciplines, which is particularly evident in fields such as computer vision and natural language processing Liu et al. (2023); Høye et al. (2021). Such models require very large datasets in order to be properly trained, i.e. minimising the loss function that represents the misfit of the data. However, the acquisition of data for many scientific and engineering problems is accompanied by considerable costs. This is particularly true in the field of climate modelling where direct numerical simulation is utilised Sivarajah et al. (2017); Kochkov et al. (2021). Consequently, there arises a pressing need for machine learning models that are capable of generalising effectively within the confines of limited data.

One approach could be using Gaussian process (GP) surrogate models, which are particularly useful in cases with limited data or noisy observations Knudde et al. (2020); Donnelly et al. (2022). Unlike other machine learning methods, that assume a specific functional form, GPs provide a flexible and adaptable way to model complex relationships in data. The main issue, nonetheless, with GPs, and generally most other deep learning models, is that they are considered black box models where the underlying process used to provide the output is not fully understandable or explainable Vakili et al. (2021); Wang et al. (2019); Chatrabgoun et al. (2022). This can be a concern in applications where understanding the reasoning or factors influencing the predictions is crucial such as climate modelling. In this case, for example, such models could provide physically impossible outputs, whilst considering it a plausible solution, which could lead to dangerous consequences if relied upon in developing mitigation strategies.

In recent years, the emergence of physics-informed machine learning (PIML) has provided a promising avenue for simulating complex dynamics while adhering to the fundamental laws governing physical systems Karniadakis et al.

(2021); Kumar et al. (2021); Mahjoubi et al. (2022). PIML represents an interdisciplinary approach that combines concepts from physics and machine learning by leveraging the representation and approximation capabilities of neural networks and integrating domain knowledge and governing physics equations into the learning process. This concept tackles both data scarcity and model explainability, which are shortcomings of deep learning and GP models.

Physics-informed neural networks (PINNs) are a specific type of PIML models that has gained significant attention as they use the physics equations as regularisation terms in the loss function thus constraining the outputs to physically consistent solutions Raissi et al. (2019). By introducing a physics loss term in the loss function, PINNs would tend to minimise both unrealistic solutions and data fitting errors. The physics loss is determined by calculating the residuals associated with the model and the physics equations. This can be done easily using Automatic Differentiation (AD) to calculate the partial derivatives of the outputs for the corresponding inputs Raissi et al. (2019).

Previously, PINN models would either heavily rely on data (e.g., as computational fluid dynamics (CFD) solutions at selected input configurations) or be trained solely based on the underlying physics equations. Both approaches may be challenged by large and complex applications, such as modelling the hydro-morphodynamics around mangrove environments. The former requires input data that is computationally expensive to generate, while the latter may fail to capture the full complexities of the region (e.g., the interactions of the mangroves with tidal waves). In this paper, we propose a novel hybrid PINNs model, which partially uses data from CFD simulations and also partially uses physics equations to constrain the predicted solutions, in order to model different fields such as elevations, velocities, and sediment dynamics around mangrove environments. By incorporating both data-driven insights and physics-based constraints, PINNs offer a promising approach to efficiently and effectively address the limitations of traditional numerical and machine learning modelling methods in capturing the complex interactions and non-linearities, present in modelling mangrove environments dynamic.

To demonstrate the effectiveness of the proposed PINNs in modelling mangrove dynamics, we conducted a case study in the Sundarbans, the world's largest mangrove forest situated between India and Bangladesh. The Sundarbans face significant climate change impacts, including sea-level rise and land erosion, making it an ideal location to investigate the potential of the PINNs in supporting ecosystem-based adaptation solutions Mukul et al. (2019). In our study, we compared the performance of PINNs against a traditional FE model that was developed to simulate the hydro-morphodynamics of mangrove environments. We focused on achieving two key aspects: decreasing computational cost and increasing accuracy.

This paper is organised as follows. In Section 2, we introduce the PINNs architecture and underlying equations. In Section 3, we introduce the region of study with its characteristics and modelling conditions to demonstrate the performance of PINNs in modelling complex dynamics around mangrove environments in real-world settings. We also compare the performance of PINNs with a traditional numerical FE model at the same region, which is recently developed in Fanous et al. (2023a). Finally, we conclude our work and discuss present limitations and possible solutions in Section 4.

2. Physics-informed neural networks

In this section, we first provide the methodology illustrated in Figure 1, where panel a) shows the numerical model used to solve Navier Stokes equations to model the hydro-morphodynamics of mangrove environments, which is briefly discussed in Section 2.1 (the full details can be found in Fanous et al. (2023a)). This numerical model was used to generate simulations over the region of interest and is required to construct the novel surrogate model proposed in this paper. Panel b) illustrates the the PINNs model including its equations, architecture, and evaluation metrics, which is developed for this complex real-world problem, over a large irregular spatial domain with complex boundary conditions. The details of this model will be discussed in Section 2.2.

2.1. Hydro-morphodynamic modelling of mangrove environments

Simulating the hydro-morphodynamics at a region of interest requires solving the Navier–Stokes (NS) equations that encompass the continuity in addition to the momentum equations Fanous et al. (2023a). Having a depth scale much smaller than the horizontal scale, it is possible to then use the depth-averaged NS, also known as the Shallow Water Equations (SWEs), as it saves on some unnecessary computational complexities.

The hydrodynamic equations of the 2D model are derived by depth-averaging from the bed, z_b, to the water surface, η. The model incorporates

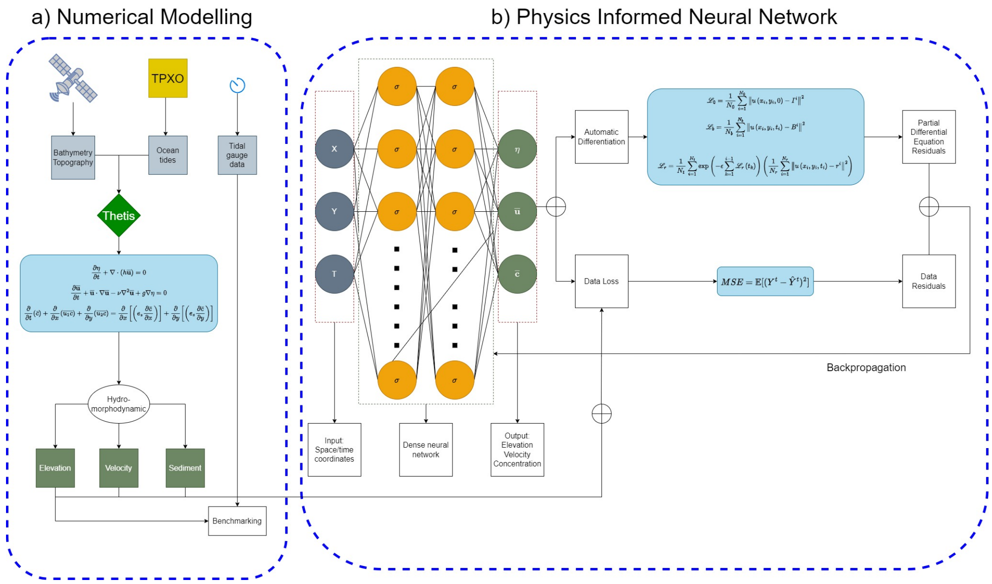

Figure 1: Proposed methodology outline

a kinematic boundary condition for the water surface, treating it as a free-moving boundary while assuming the impermeability of the bed, i.e., water does not pass through it. Therefore, the nonlinear SWEs used in this model can be expressed as follows:

$$\frac{\partial \eta}{\partial t} + \nabla \cdot (h\overline{\mathbf{u}}) = 0, \tag{1}$$

$$\frac{\partial \overline{\mathbf{u}}}{\partial t} + \overline{\mathbf{u}} \cdot \nabla \overline{\mathbf{u}} - \nu \nabla^2 \overline{\mathbf{u}} + g \nabla \eta = 0, \tag{2}$$

where, $h = \eta - z_b$ represents the depth, ν denotes the turbulent kinematic eddy viscosity, and $\overline{\mathbf{u}}$ is the depth-averaged velocity vector, and its components, $\overline{u}_1$ and $\overline{u}_2$, correspond to the flow in the x and y directions, respectively (refer to Fanous et al. (2023a) for further details).

Regarding the morphodynamics, we adopt an Eulerian approach, which considers the concentration of sediment particles and determines sediment dynamics using an advection-diffusion equation. By combining diffusion and dispersion effects over a prolonged sedimentation process, the depth-averaged sediment concentration is given by:

$$\frac{\partial}{\partial t}(\bar{c}) + \frac{\partial}{\partial x}\left(\overline{u_1 c}\right) + \frac{\partial}{\partial y}\left(\overline{u_2 c}\right) = \frac{\partial}{\partial x}\left[\left(e_s \frac{\partial \bar{c}}{\partial x}\right)\right] + \frac{\partial}{\partial y}\left[\left(e_s \frac{\partial \bar{c}}{\partial y}\right)\right] \quad (3)$$

Here, $\bar{c}$ represents the sediment concentration, e_s denotes the sediment turbulent diffusivity coefficient, given by $e_s = v_s^h/\sigma_s$, where v_s^h represents the horizontal viscosity, and σ_s stands for the turbulent Schmidt number.

In order to solve the above equations, we developed a two-dimensional coupled hydro-morphodynamic model within *Thetis*, a finite element model for simulating coastal and estuarine flows. The main advantage of using *Thetis* is that it uses a discontinuous Galerkin (DG)-based finite element discretisation, which is proven to be robust for solving NS problems Fehn et al. (2018). DG employs an unstructured mesh composed of triangular elements for tessellation, upon which a FE space is established. The representation of variables within a discontinuous space involves solving for the variables along element edges. Due to its suitability for advection-dominated problems and its ability to handle unstructured meshes, which are particularly important for irregular geometries in coastal areas, this approach has gained significant interest in hydro-morphodynamic applications Weinberg and Wieners (2021).

A semi-implicit Crank-Nicolson time-stepping method is employed to ensure second-order accuracy and computational efficiency. This approach requires only one non-linear solution per time-step, contributing to faster execution. Furthermore, this particular time integration scheme minimises excessive dissipation of tidal waves, preserving the solutions' characteristics without excessively smoothing them, unlike the fully implicit backward Euler method Fanous et al. (2023a).

In order to avoid some instabilities in the numerical model, as a result of not reaching a stable flow state at the beginning of the simulation, which may result in unrealistic sediment changes, we initialise the model first by spinning the hydrodynamics. Once the elevation and velocity fields have reached a steady state, we introduce then the morphodynamic equations (see Fanous et al. (2023a) for further details).

Using an unstructured mesh and a semi-implicit time-stepping method, we provide the numerical model with appropriate time and space-varying conditions to describe the settings at the region of interest so that the model can accurately simulate the hydro-morphodynamics.

2.2. PINNs model

The solutions to partial differential equations (PDEs) can be generally represented in the following form:

$$u_t + \mathscr{N}[u; \lambda] = 0, \quad \mathbf{x} \in \Omega, \quad t \in [0, T] \tag{4}$$

Here, $u(t, \mathbf{x})$ represents the solution, and $\mathscr{N}[.; \lambda]$ is a general linear or nonlinear operator with system parameters λ. The variables t and $\mathbf{x}$ correspond to the time and spatial inputs of the system, respectively. The spatial domain Ω can be bounded based on prior knowledge of the dynamical system, and $[0, T]$ denotes the time interval over which the system evolves. To properly define the problem and solve Equation (4), it is typically necessary to specify initial conditions $u(\mathbf{x}, 0)$ and/or boundary conditions $u(\mathbf{x}^0, t^0)$.

This general form encompasses a wide range of problems, where $\mathscr{N}$ can be parabolic, hyperbolic, or elliptic, representing fluid dynamics, heat conduction, or steady-state diffusion, respectively.

For a two-dimensional problem, following Raissi et al. (2019), the function $u(x, y, t)$ is approximated using a fully connected network denoted as $f(x, y, t)$. This network takes the coordinates (x, y, t) as inputs and provides the corresponding outputs $u_{\mathscr{N}}(x, y, t)$. Then, by using AD, we can back-propagate from the outputs to the inputs to calculate the partial derivatives in terms of both time and space coordinates, i.e. $\frac{\partial u}{\partial x}$ or $\frac{\partial u}{\partial t}$. A residual is calculated between the calculated partials of $f(x, y, t)$ and equation partials $u(x, y, t)$, which will be added as an equation loss term in the loss function. Hence, $f(x, y, t)$ and $u(x, y, t)$ have shared parameters, but with different activation functions, which is attributed to the inclusion of the differential operator $\mathscr{N}$. The main advantage of using AD is its ability to calculate the exact derivatives, thus eliminating the descritisation error.

The structure of the explained PINNs model is shown in Figure 2, compromising of a fully connected neural network with multiple hidden layers with each hidden neuron containing a weight $w_{i,j}$, bias b_j, and a nonlinear activation function σ such as hyperbolic tangents, ReLUs, leaky ReLUs, ELUs or Swish Bihlo and Popovych (2022).

The neural network parameters are learned by minimising the mean squared error (MSE) loss, which is defined as follows:

$$\mathscr{L} = \mathscr{L}_0 + \mathscr{L}_b + \mathscr{L}_r, \tag{5}$$

where

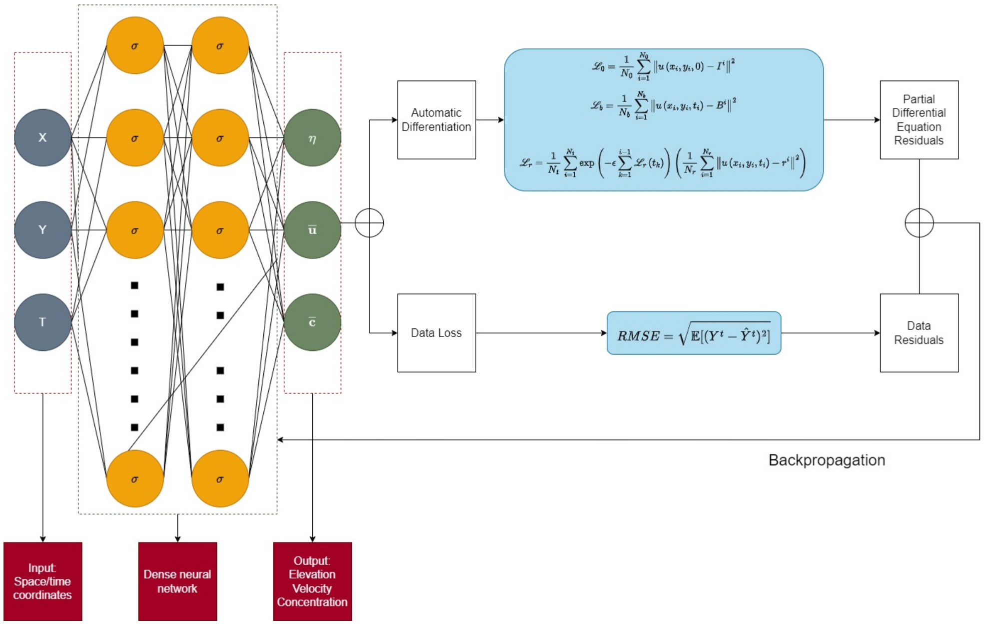

Figure 2: **Physics-informed neural network (PINN) architecture.** The inputs to the network are the time and space coordinates, which are passed through a deep fully connected neural network to obtain the desired quantities of interest such as water elevation (η), velocity ($\overline{\mathbf{u}}$) in both x and y directions, and sediment concentration ($\overline{\mathbf{c}}$). Then, gradients of the network's output with respect to its input are computed at these locations using automatic differentiation. Finally, the residual of the underlying differential equation is computed using these gradients and added as an extra term in the loss function in addition to the data loss.

$$
\begin{aligned}
\mathscr{L}_0 &= \frac{1}{N_0}\sum_{i=1}^{N_0}\left\|u\left(x_i, y_i, 0\right) - I^i\right\|^2 \\
\mathscr{L}_b &= \frac{1}{N_b}\sum_{i=1}^{N_b}\left\|u\left(x_i, y_i, t_i\right) - B^i\right\|^2 \\
\mathscr{L}_r &= \frac{1}{N_r}\sum_{i=1}^{N_r}\left\|u\left(x_i, y_i, t_i\right) - r^i\right\|^2
\end{aligned}
\tag{6}
$$

In these equations, $\mathscr{L}_0$, $\mathscr{L}_b$, and $\mathscr{L}_r$ represent the initial loss, boundary loss, and residuals of the governing equations, respectively. These losses are computed using a finite set of collocation points. These points are sampled uniformally, although there are different sampling strategies that could be implemented as well, across the domain and constitute the location where the solutions of the PINNs model is compared against the actual solutions of the numerical model Raissi et al. (2019); Daw et al. (2022). Furthermore, I^i, B^i, and r^i correspond to the initial, boundary, and domain solutions at these collocation points, respectively. Finally, N_0, N_b, N_r are the number of points at these domains. The obtained residuals are minimised by adjusting the neural network parameters through optimisation algorithms such as Adam or L-BFGS-B, which utilise gradient descent or quasi-Newton methods, respectively Cuomo et al. (2022).

While PINNs provide promising alternatives for numerical models, the standard formulation explained above fails to capture complex multi-scale high nonlinear solutions Monaco and Apiletti (2023). This is due to the model minimising all losses $\mathscr{L}_.$ simultaneously even if predictions at previous time are inaccurate Wang et al. (2022). This would inevitably violate the temporal causality, and thus lead to errors especially for time-dependent PDEs. In order to avoid this issue, Wang et al. (2022) suggest reducing the emphasis on subsequent time steps. In pursuit of this objective, the authors reformulate the residual term as a weighted combination of residual losses calculated at a fixed time step using the following equation:

$$\mathscr{L}_r = \frac{1}{N_t} \sum_{i=1}^{N_t} w_i \mathscr{L}_r\left(t_i\right) \tag{7}$$

where N_t is the temporal descritisation, and the weights w_i would have large enough values to enable the minimisation of $\mathscr{L}_r\left(t_i\right)$ upon the condition if all previous residuals $\{\mathscr{L}_r\left(t_k\right)\}_{k=1}^{i-1}$ prior to t_i are suitably minimised. To achieve this, the weights w_i would be defined as the following:

$$w_i = \exp\left(-\epsilon \sum_{k=1}^{i-1} \mathscr{L}_r\left(t_k\right)\right) \tag{8}$$

where ϵ is the temporal causality parameter, controlling the steepness of the weights w_i. Consequently, the reformulated residual loss term can be written as follows:

$$\mathscr{L}_r = \frac{1}{N_t} \sum_{i=1}^{N_t} \exp\left(-\epsilon \sum_{k=1}^{i-1} \mathscr{L}_r\left(t_k\right)\right) \mathscr{L}_r\left(t_i\right). \tag{9}$$

Defining w_i as an inversely exponential related to the magnitude of the cumulative residual loss from previous time steps ensures that $\mathscr{L}_r(t_i)$ will not be minimised unless all previous residuals $\{\mathscr{L}_r(t_k)\}_{k=1}^{i-1}$ decrease to a small value such that w_i is sufficiently large.

In addition to introducing the causality weighted loss, we introduce a data loss term $\mathscr{L}_{data}$ which will account for the residual between the predicted and actual output, where the latter would come from the CFD simulation. The motivation behind the data loss term is that the interaction between the mangrove dynamics and incoming tidal waves are not fully accounted for in Equations (1) and (2). Thus, the modified loss equation would become:

$$\mathscr{L} = \mathscr{L}_0 + \mathscr{L}_b + \mathscr{L}_r + \mathscr{L}_{data}, \tag{10}$$

To properly capture such interactions, it would require defining spatially varying parameters such as Manning's friction coefficient, kinematic viscosity, and varying bed levels which could significantly increase the training time for the PINNs model (see Fanous et al. (2023a) for details about these parameters). Therefore, we utilise a small dataset from the numerical simulation output to train the PINNs on the elevation and velocity fields, while the sediment concentration is inferred purely from the physics equations, i.e., from Eq.3. Consequently, this becomes a hybrid data and physics driven PINNs model, which would result in faster training and convergence times than regular PINNs.

2.3. Model setup

Our PINNs model is constructed using the NVIDIA Modulus framework (see details about this Modulus, mod), which is a PyTorch-based neural network framework designed for PINNs. The PINNs model we developed consists of six fully connected multi-layer perceptron architectures, each comprising 256 neurons, and utilises the "swish" activation function. The swish activation function, defined by the following equation

$$\phi(x) = \frac{x}{1 + e^{-x}}, \tag{11}$$

which is a smooth non-monotonic function that has demonstrated improved performance over ReLU in deeper models Ramachandran et al. (2017).

To incorporate boundary and initial conditions into the PINNs, we sampled points both on the domain boundary and in the interior. We employed the *Adam* optimiser and utilised an exponentially decaying learning rate of

0.95 per 100,000 iterations for a total of 1,000,000 iterations and with a batch size of 512. An L_2 regularisation (sum of squares error) was applied to measure the approximation error of the neural network, which was minimised using the Adam optimiser Raissi et al. (2019).

To assess the performance and evaluate the accuracy of the constructed PINNs model, a comprehensive validation process was conducted by comparing its predictions with the simulation data obtained from *Thetis*. The comparison was carried out at multiple time-steps, specifically at 12, 16, 20, and 24 hours, which show the spatial and temporal evolution of the model under different tidal stages (i.e., beginning of the tide, tidal peak, and end of tide).

The model simulation period was chosen from June 30, 2013, to July 1, 2013, due to the availability of reliable tidal gauge records. Furthermore, the numerical model was validated against this tidal data to ensure that the model is accurate and can be used as validation against the output of the PINNs model Fanous et al. (2023a).

2.4. Performance metrics

In order to asses the model's predictive performance, the root mean squared error (RMSE) was employed as a performance metric to assess the predictive capability of the model for elevation, $\overline{u}_1$ and $\overline{u}_2$ velocities, and concentration outputs at times 12, 16, 20, and 24 hours. It is calculated using the equation:

$$\mathrm{RMSE} = \sqrt{\mathbb{E}\left[(\mathbf{y} - \hat{\mathbf{y}})^2\right]}, \tag{12}$$

where $\mathbf{y}$ represents the actual output obtained from the numerical simulation, and $\hat{\mathbf{y}}$ corresponds to the predicted output from the PINNs model.

The selection of the RMSE as the evaluation metric in this study is due to its ability to provide interpretable results by scaling the prediction errors back to the original unit of measurement, which in this case is expressed in meters [m].

In addition to providing RMSE values of the outputs (i.e., elevations at both directions and sediment concentrations) at the mentioned time-steps, we will illustrate the actual, predicted and their differences of these outputs at the time-steps over the entire spatial domain in Section 3.2. These images could be also used to examine the predictive performance of the proposed method in this paper.

3. Case Study: PINNs for modelling Sundarbans mangroves

In this section, we introduce the computational domain used to model the hydro-morphodynamics around mangrove environments at the Sundarbans. Then, we demonstrate the performance of the developed PINNs model and discuss its results and suitability as a surrogate when compared against the numerical solver.

3.1. Computational domain

The geographical extent of the model encompasses the complete shelf area of the Bay of Bengal, as well as the Sundarbans mangrove forest that straddles the border of India and Bangladesh. The spatial coverage of this region is illustrated in Figure 3.

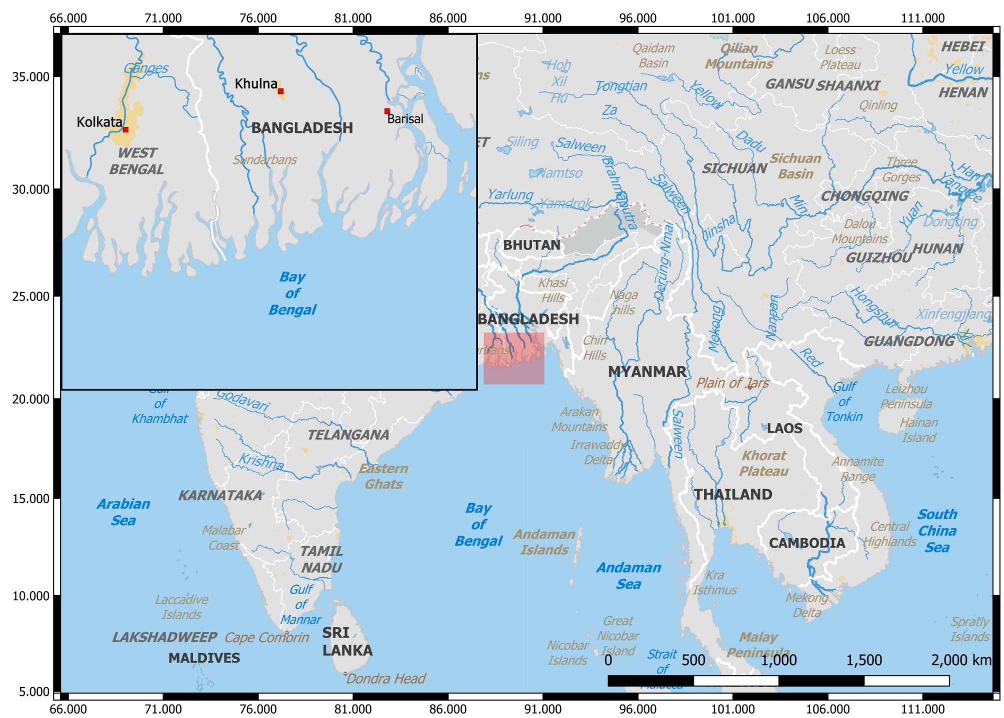

Figure 3: Geographical location of the Sundarbans

We developed a spatially varying mesh resolution to capture the dynamics of the tidal waves from the Indian Ocean up until the Sundarbans mangroves. The resolution of the domain varied from 8 km deep at the Ocean to 1.5 km at the mangroves site. The generated mesh is shown in Figure 4. The resultant mesh has over 125,000 cells with spatially varying resolutions.

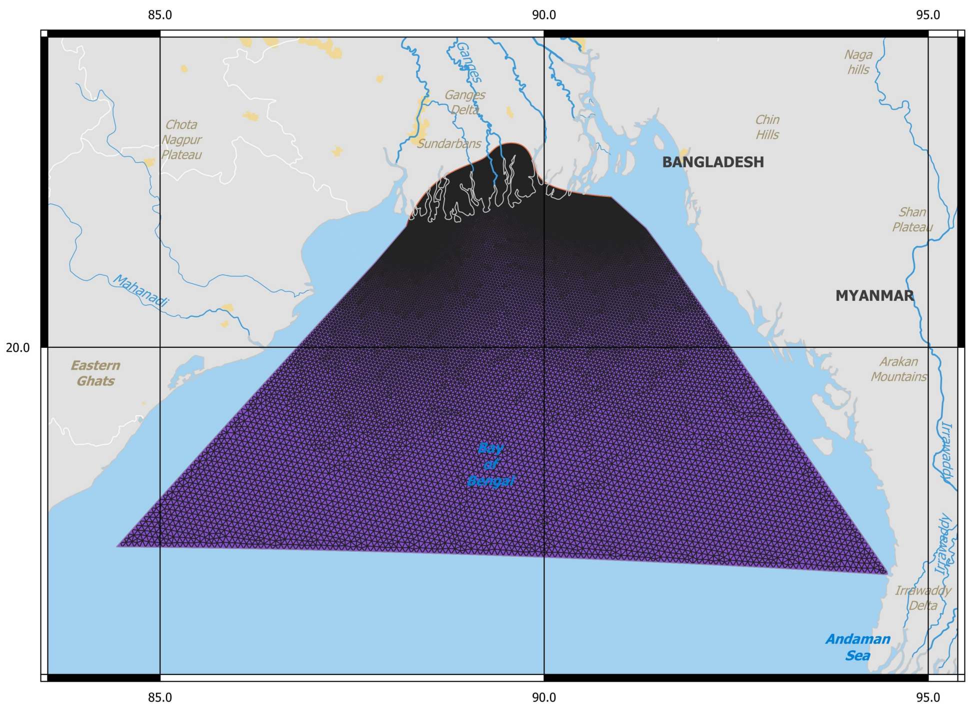

Figure 4: Mesh generated using Gmsh with varying resolution from 1.5 km to 8 km

In order to account for the absence of topography/bathymetry in the PINNs model, we incorporated the effect of mangroves at the land border by imposing a no-slip condition, where both horizontal velocities ($\overline{u}_1$ and $\overline{u}_2$) are set to zero. Similarly, to ensure comparability with the numerical solver, we enforced the same boundary condition at the land boundary.

Furthermore, to simulate tidal waves, we implemented a periodic boundary condition at the sea, which introduces a tidal elevation using the following equation:

$$\text{Elevation} = A \sin\left(\frac{2\pi t_l}{T}\right), \tag{13}$$

where A represents the tidal amplitude, t_l is the simulation time, and T denotes the tidal period. For our model, we selected A to be 1 m and set T

to 12 hours, which corresponds to a semi-diurnal tidal wave pattern observed in the Bay of Bengal.

Finally, in addition to the no-slip boundary conditions imposed at the land boundary, we imposed spatially varying Manning's coefficient to simulate the effect of mangrove environments. To explain, at the mangrove region, a Manning's value of 0.15 was set that represents a dense forest Fanous et al. (2023a). However, moving towards the sea boundary, the value of Manning's coefficient decreases reaching 0.001 as the friction is negligible deep in the Ocean.

3.2. Results

Running the PINNs model took approximately 24 hours in real time, which is significantly faster when compared to the numerical FE model that took approximately five days between hydrodynamic spin-up and full simulation. Such increase in the computational speed is critical, as discussed in Section 1, to increase the success rate of protection and mitigation projects when faced with different climate events.

With regards to the training loss of the model, Figure 5 shows the change of the log aggregated loss as the number of iterations increase. From Figure 5, it can be noticed that the loss decreases remarkably during the first 200,000 iterations. From there, the loss almost stabilises with minimal decreases over the rest of the iterations. Furthermore, the loss appears to be decreasing in a stable manner, which proves the training stability of the PINNs model.

To quantify the model's accuracy, we compared the results of the PINNs model with those of the numerical model, and Table 1 shows the RMSE scores of the elevation, $\overline{u}_1$-velocity and $\overline{u}_2$-velocity, and concentration at different times of the simulation. From Table 1, it can be seen that the PINNs model performs very well over all fields and across different simulation times. This shows that the model is able to accurately capture the change in the hydrodynamics as well as the morphodynamics (sediment transport) across different stages of the tidal cycle.

Finally, spatial illustrations in Figures 6 - 9 visualise the prediction power of PINNs when compared to that of the numerical model for all outputs at the same time snapshots of Table 1. From Figures 6 - 8, the ability of mangroves to attenuate incoming tidal waves is clearly visible. The mangrove reduced tidal heights and velocities almost entirely, and the region at the land border does not have any significant tidal heights or velocities left. Furthermore, the PINNs model was able to regenerate the complex tidal structure and

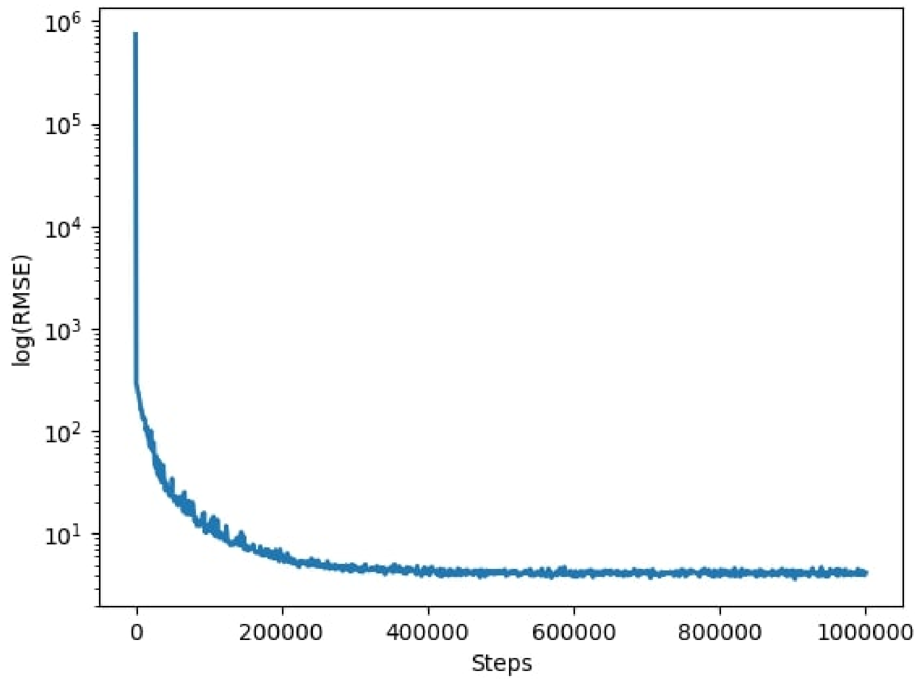

Figure 5: Training of PINNs model with y-axis showing the log(RMSE) loss and x-axis showing the training steps

.

the interaction between mangrove environments and the tides. This also demonstrates the importance of adding the temporal causality. Without this causality, the PINNs model would not have been properly trained for the initial conditions at the region, which could result in significant errors, as the initial structure is critical for determining the interaction for the rest of the tidal cycle.

With respect to Figure 9, the output clearly shows the ability of mangrove environments to prevent entirely any sediment erosion. The change in sediment concentration over time is barely visible and just seen at the interface of the incoming tides and mangrove region. It is important to note here that the PINNs model did not predict the very small concentration change at this interface. This is possibly due to the change being minimal, i.e. in the order of e^{-6} and less, and the PINNs model focusing on higher losses in

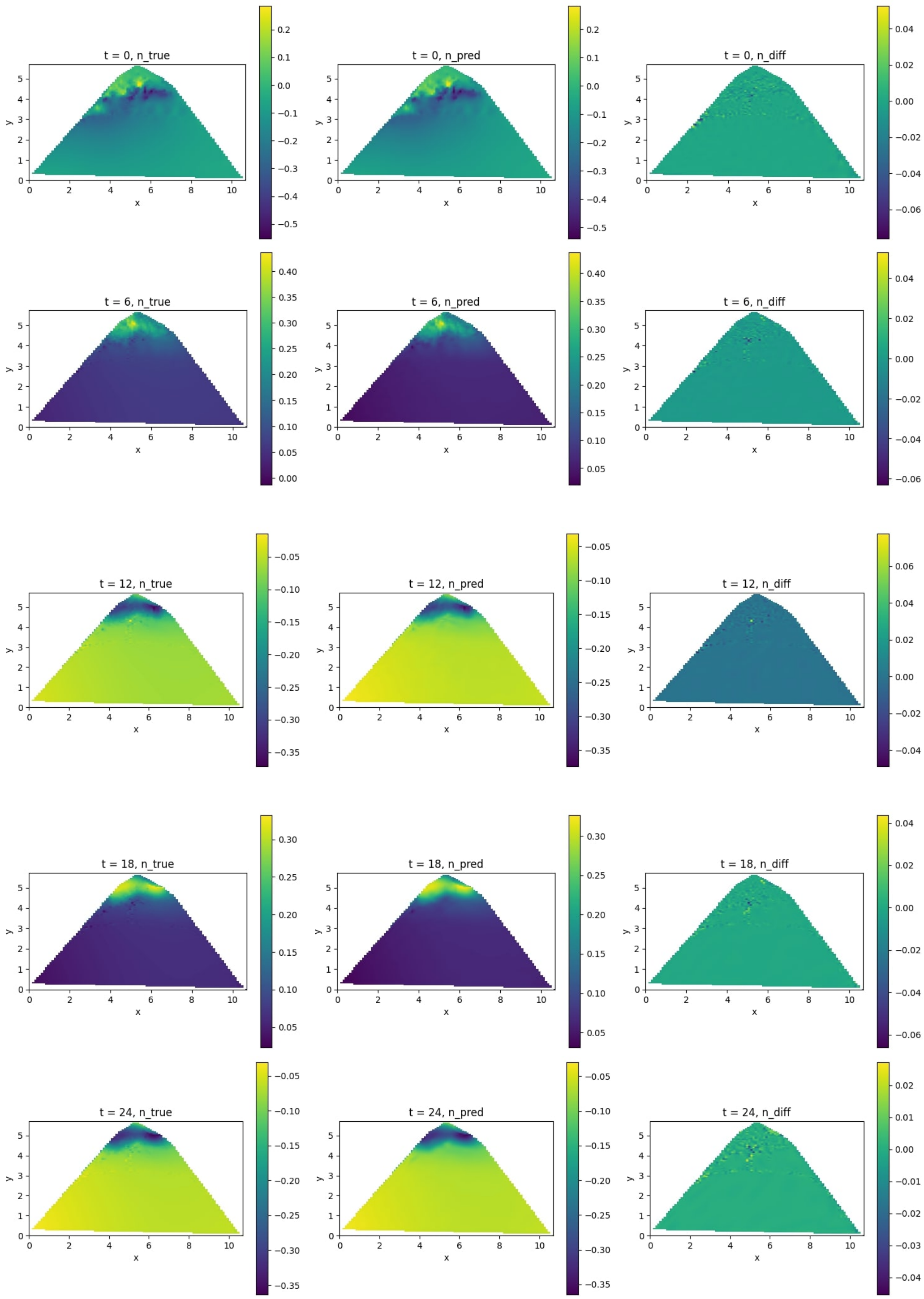

Figure 6: Actual vs predicted elevation at times 0, 6, 12, 18, and 24 hours.

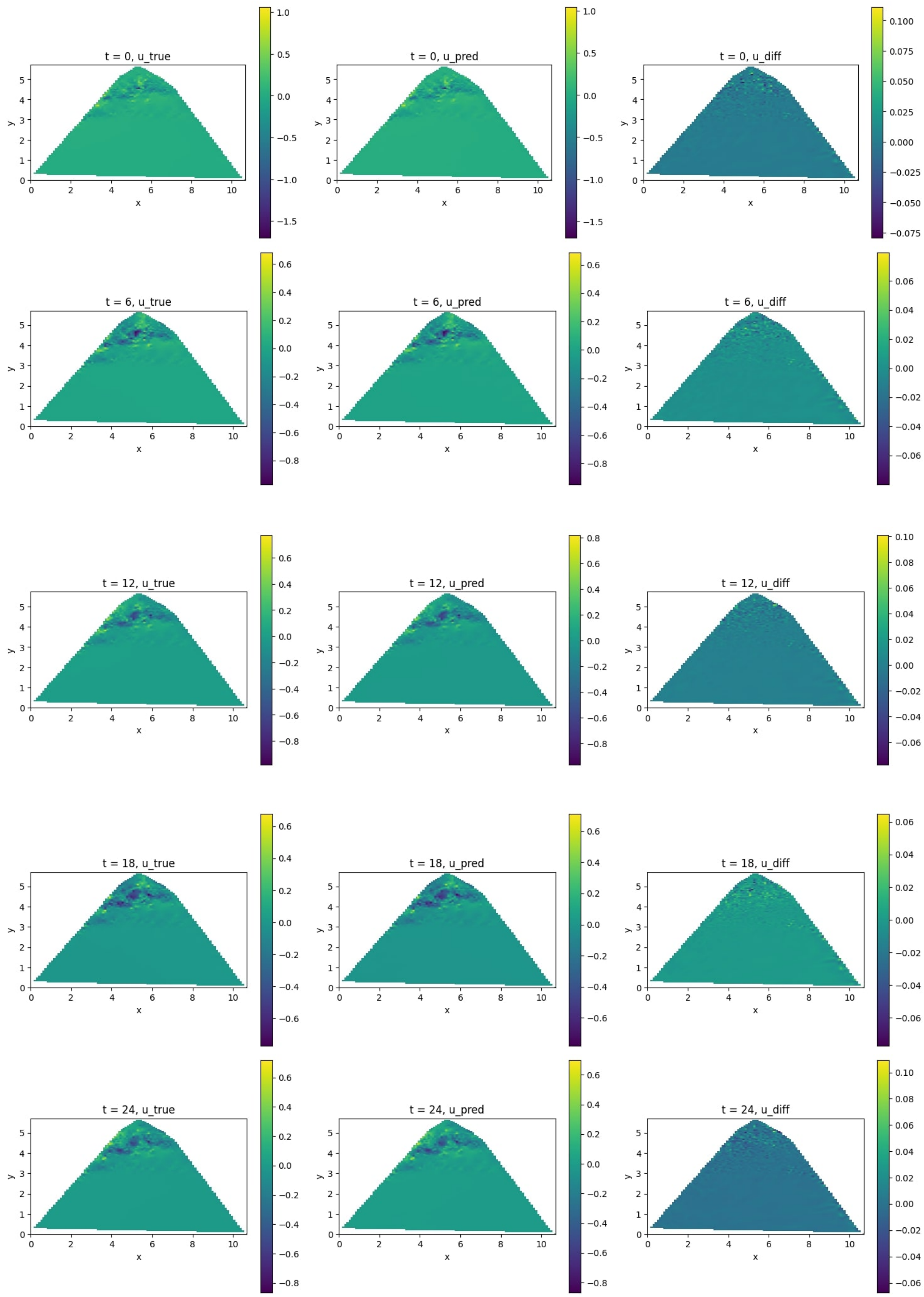

Figure 7: Actual vs predicted $\overline{u}_1$-velocity at times 0, 6, 12, 18, and 24 hours.

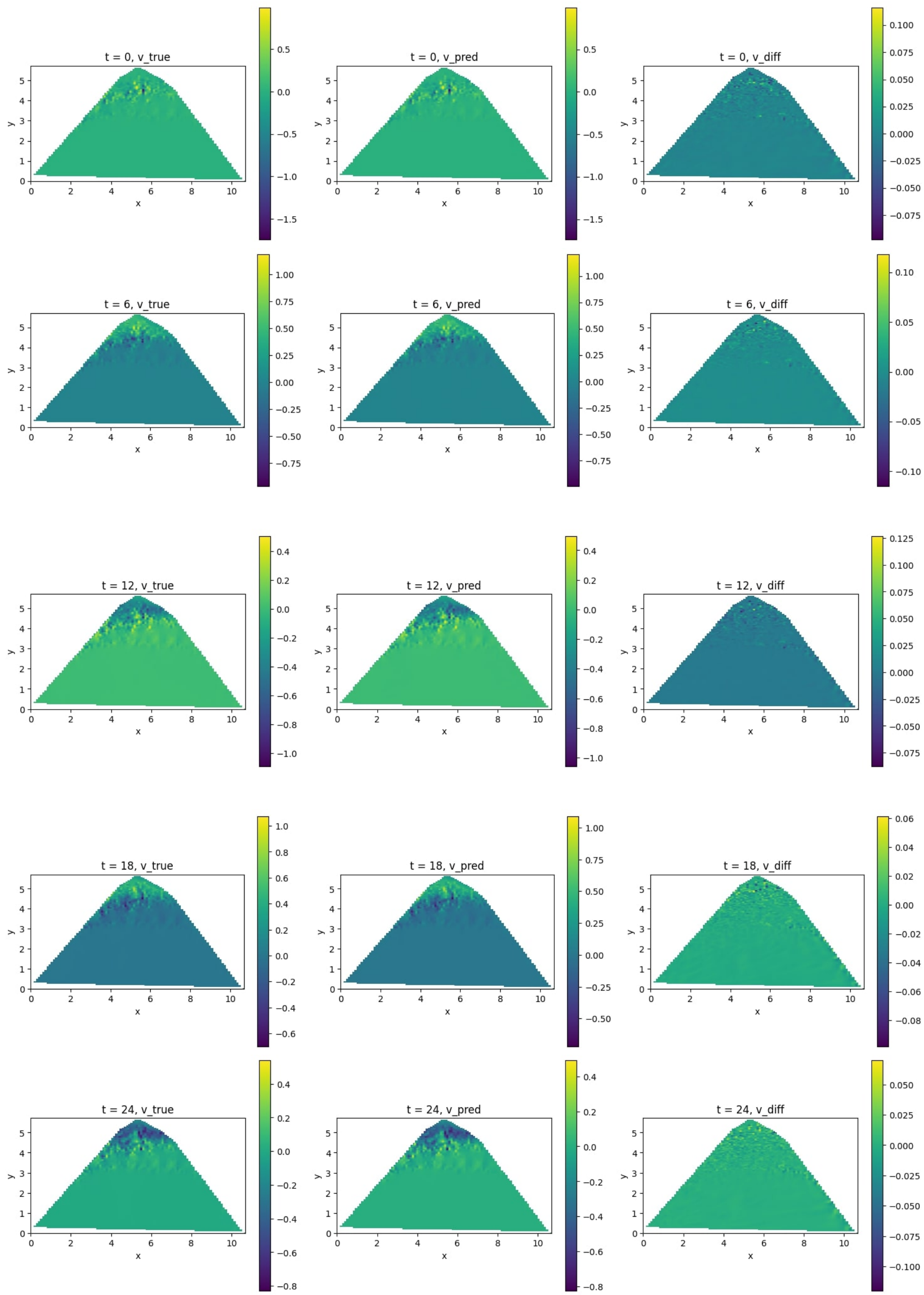

Figure 8: Actual vs predicted $\overline{u}_2$-velocity at times 0, 6, 12, 18, and 24 hours.

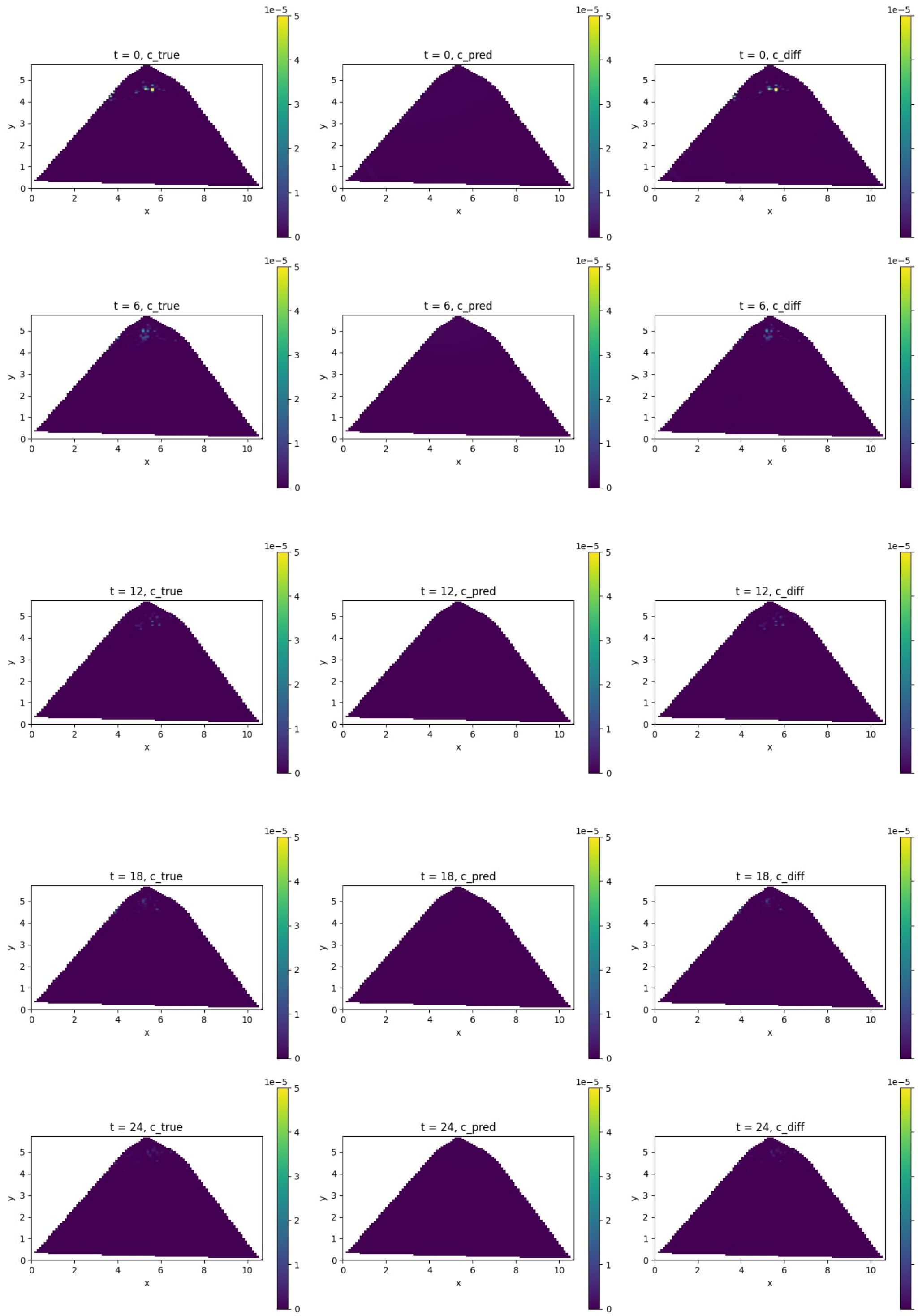

Figure 9: Actual vs predicted concentration at times 0, 6, 12, 18, and 24 hours.

Table 1: RMSE values for elevation, $\overline{u}_1$-velocity, $\overline{u}_2$-velocity, and concentration of PINNs against FE model/Thetis Fanous et al. (2023b)

Time (hours)	**Elevation**	$\overline{u}_1$**-velocity**	$\overline{u}_2$**-velocity**	**Concentration**
0	0.008	0.023	0.023	6.23e-06
6	0.007	0.017	0.02	2.12e-06
12	0.007	0.016	0.019	1.11e-06
18	0.006	0.015	0.018	1.25e-06
24	0.007	0.016	0.02	7.51e-07

the elevation and velocities. Nevertheless, the outputs still demonstrate the model's ability in predicting that almost no sediment change is happening at the domain.

Thus, the figures illustrate the remarkable accuracy of the PINNs model and its ability to handle complex interactions in large domains with complex boundary conditions. The PINNs model was able to replicate with very high accuracy the hydro-morphodynamic outputs simulated by the numerical model without needing to solve the complex physics equations. In terms of computational efficiency, the PINNs model, as discussed at the beginning of the section, was considerably faster than the numerical model when training the latter for initial and boundary conditions in addition to some simulation data taken from the numerical model. Moreover, for providing inference at unseen data-points, the model was substantially faster as it took less then 15 seconds to provide its predictions for the outputs fields. This is not possible in the numerical model as it has to rerun the whole simulation again, which is impractical in real-world cases where the speed of getting the information is crucial for effective and quick decision making by the local and governmental entities at the region.

It could be argued that the PINNs model used some numerical simulation data for training, thus there is an inevitable computational demand for running the numerical model first. However, as with any machine learning, once the model is properly trained, i.e. converged to an acceptable loss, the model does not have to be retrained again. In fact, just providing the new conditions, the PINNs model would then be able to immediately predict the output as long as the conditions were not significantly changed to the ones used in training. This concept is present in all machine learning models, where if the testing data is quite different to the data trained on, the model's accuracy and performance would deteriorate. In our case, the model would be able to perform well on similar tidal and mangrove boundary conditions, which are normally present in this region. Nonetheless, if one wants to incorporate not only daily changes but also seasonal and annual dynamics, it would be possible to achieve performance comparable to the current model by training the PINNs model on appropriate time scales. Since the model is meshless, it does not require solving these equations in any spatial or time domains.

4. Conclusion

Quantifying the role of mangrove environments in attenuating waves, preventing erosion, and providing ecosystem-based adaptation solutions is crucial for effective risk assessment, informed decision-making, and mitigating climate change impacts. Understanding the extent of these services enables scientists, policymakers, and stakeholders to make informed choices regarding coastal development, land-use planning, and infrastructure design, while also protecting natural ecosystems, biodiversity, and fragile habitats. Recognising the importance of mangroves in coastal areas is key to fostering sustainability, environmental management, and ensuring a sustainable future for both coastal ecosystems and neighbouring communities.

The proposed machine learning model provides a fast and accurate alternative to traditional numerical models, which could be critically important for real-time predictions and assessment of current climate conditions at the region of study. This paper uses novel machine learning methods to model the hydro-morphodynamics of mangrove environments for an expansive region with real complex boundary conditions. The approach involves developing a hybrid data and physics-informed neural network (PINNs) and a custom loss function that accounts for temporal causality when training the model. This would ensure accurate modelling of mangrove environments and their ability in attenuating waves and preventing erosion due to their complex root structure. Furthermore, the temporal causality factor addresses the shortcomings of vanilla PINNs (consisting of a fully connected deep neural network and physics loss function) by forcing the model to converge on initial conditions before reducing the losses for upcoming temporal discretisations.

The developed model has several advantages over traditional deep learning models. One key advantage is its ability to incorporate known physical laws into the learning process by enforcing the governing equations and boundary conditions as constraints during training. This leads to more accurate and physically consistent predictions over other deep learning models. Moreover, PINNs are data efficient as they require fewer training data points compared to traditional models since they effectively learn from limited data and extrapolate predictions to unseen scenarios. Finally, PINNs can handle irregular domains and complex geometries more effectively, making them suitable for a wide range of applications. To explain, traditional deep learning models often require structured and evenly sampled data, which can be challenging when dealing with irregularly shaped domains or complex geometries. By incorporating the governing equations and boundary conditions as constraints during training, PINNs can capture the behaviour of the system even in regions with sparse or irregularly distributed data.

The results of the study demonstrate the suitability of the developed PINNs model as an effective surrogate when compared to a finite element numerical model. The RMSE of all output fields, including elevation, velocity in both x and y directions, and sediment concentration, were between e^{-2} and e^{-3}. The model was also consistent for different stages of the tidal cycle, i.e. beginning of the tide, tidal peak, and end of tide as demonstrated in the figures in Section 3.2. This shows the robustness of the developed model and its flexibility in modelling different complex interactions between the incoming tidal waves and the mangrove environments. Furthermore, with regards to mangrove environments, the results showed their ability to attenuate most of the tidal heights and its velocity, in addition to preventing almost any sediment change where such changes were barely visible.

Computational efficiency was also a key element in showing the superiority of the PINNs model compared to the numerical model. The training time of the PINNs model was about 24 hours for 1,000,000 iterations although the model mostly converged after approximately 200,000 iterations. This is significantly faster than the numerical solver, which took approximately 5 days to simulate the same period including hydrodynamic spin-up to prevent model instabilities.

Using a hybrid data and physics-driven approach for the PINNs model has some computational costs that we need to consider. Modelling the interactions of mangrove environments and the complex dynamics associated with them is non-trivial and requires extensive modifications to the Navier–Stokes equations. This makes the training procedure of the PINNs model more difficult, demanding a significant increase in training time. Thus, utilising a hybrid approach, where some data from numerical simulations is used to aid the PINNs model in modelling such complex processes, eases the computational cost of the latter but inevitably requires some numerical simulation to run. Although this increases the overall cost in general, once sufficiently trained, i.e. the cumulative loss is reduced to an acceptable level, there is no further requirement for additional numerical simulation data for prediction and conducting inference at testing points, as the network parameters have been optimised. This makes the inference process at “unseen” data-points incredibly fast, taking just few seconds. The numerical model, in contrast, requires running the full simulation again, which is computationally very expensive, particularly for the applications discussed in this study. As a result, the associated training cost for the PINNs model depends on the objective of the steady, i.e. determining daily, monthly, seasonal, or decadal trends, and in all cases prediction cost would be negligible.

While the developed PINNs model in this study focused on mangrove environments, the methodology described can be extended to model other coastal ecosystems (e.g., marshes) and even generalise to any problem involving simulating hydrodynamics and morphodynamics. The only difference would be in the data-driven part of the PINNs model, which requires some simulations for the selected case. This demonstrates the potential of the developed hybrid data and physics-driven PINNs, in addition to the modified temporal weighted loss, to be applied to a wide range of problems where the underlying physics of the domain can be described using Navier–Stokes equations.

Such flexibility of the proposed PINNs model can also be observed in training on different time scales. In this study, we trained the PINNs model to infer daily interactions of the mangrove environments and the tidal waves. Nonetheless, it is possible to expand the time scale to capture weekly, seasonal, and even yearly trends. This would mainly depend on the intended objective from building such models. Furthermore, this would mean some increase in the computational cost driven by the need of more simulation data to train the PINNs model. However, the inferencing time for such large time scale applications would be immeasurable compared to traditional numerical modelling. Future works should consider modelling real extreme climate events such as tropical cyclones using PINNs. These events pose significant challenges due to their intricate dynamics and interactions with the environment posing significant threats to the coastal communities. Leveraging PINNs has the potential to provide huge advantages especially when real-time monitoring and evaluation is required in order to implement immediate protection and mitigation strategies to save the lives of people living in those areas and preserve the natural ecosystems.

Furthermore, an important limitation of PINNs is the lack of a direct approach to uncertainty quantification using a Bayesian paradigm. Quantifying uncertainty is crucial in many scientific and engineering applications, as it provides valuable insights into the reliability and confidence of the model's predictions. While quantifying uncertainty could be done using sampling techniques, such as Monte Carlo, this limits the ability to propagate uncertainty from the inputs to the outputs, thus omitting valuable information when quantifying the confidence of the model in predicting the output fields. Future works could address this limitation by incorporating Gaussian Processes into the framework of PINNs, or as a standalone complementary procedure after training the PINNs model, would significantly enhance their practical utility and provide robust quantification of predictive uncertainty.

Acknowledgements

The authors would like to thank Coventry University for funding this PhD Studentship titled "Enhancing Mangrove Forest Resilience against Coastal Degradation and Climate Change Impacts using Advanced Bayesian Machine Learning Methods", through the GCRF Scheme.

References

, . Modulus — NVIDIA Developer. URL: https://developer.nvidia.com/modulus.

Bihlo, A., Popovych, R.O., 2022. Physics-informed neural networks for the shallow-water equations on the sphere. Journal of Computational Physics 456, 111024. doi:http://dx.doi.org/10.1016/J.JCP.2022.111024, arXiv:2104.00615.

Chatrabgoun, O., Esmaeilbeigi, M., Cheraghi, M., Daneshkhah, A., 2022. Stable likelihood computation for machine learning of linear differential operators with gaussian processes. International Journal for Uncertainty Quantification 12.

Cooley, S., Schoeman, D., Bopp, L., Boyd, P., Donner, S., Ghebrehiwet, D., Ito, S.I., Kiessling, W., Martinetto, P., Ojea, E., Racault, M.F., Rost, B. and, ., Skern-Mauritzen, M., 2022. Ocean and coastal ecosystems and their services, in: Pörtner, H.O., Roberts, D.C., Tignor, M., Poloczanska, E.S., Mintenbeck, K., Alegría, A., Craig, M., Langsdorf, S., Löschke, S., Möller, V., Okem, A., Rama, B. (Eds.), Climate Change 2022: Impacts, Adaptation and Vulnerability. Contribution of Working Group II to the Sixth Assessment Report of the Intergovernmental Panel on Climate Change. Cambridge University Press, Cambridge, UK and New York, NY, USA. book section 3. URL: https://www.ipcc.ch/report/ar6/wg2/downloads/report/IPCC_AR6_WGII_Chapter03.pdf, doi:http://dx.doi.org/10.1017/9781009325844.005.

Cuomo, S., Di Cola, V.S., Giampaolo, F., Rozza, G., Raissi, M., Piccialli, F., 2022. Scientific Machine Learning Through Physics–Informed Neural Networks: Where we are and What's Next. Journal of Scientific Computing 2022 92:3 92, 1–62. URL: https://link.springer.com/article/10.1007/s10915-022-01939-z, doi:http://dx.doi.org/10.1007/S10915-022-01939-Z, arXiv:2201.05624.

Daw, A., Bu, J., Wang, S., Perdikaris, P., Karpatne, A., 2022. Mitigating Propagation Failures in Physics-informed Neural Networks using Retain-Resample-Release (R3) Sampling URL: https://arxiv.org/abs/2207.02338v3, arXiv:2207.02338.

Donnelly, J., Abolfathi, S., Pearson, J., Chatrabgoun, O., Daneshkhah, A., 2022. Gaussian process emulation of spatio-temporal outputs of a 2d inland flood model. Water Research 225, 119100.

Fanous, M., Daneshkhah, A., Eden, J.M., Remesan, R., Palade, V., 2023a. Hydro-morphodynamic modelling of mangroves imposed by tidal waves using finite element discontinuous Galerkin method. Coastal Engineering 182, 104303. doi:http://dx.doi.org/10.1016/J.COASTALENG.2023.104303.

Fanous, M., Eden, J.M., Remesan, R., Daneshkhah, A., 2023b. Challenges and prospects of climate change impact assessment on mangrove environments through mathematical models. Environmental Modelling Software 162, 105658. doi:http://dx.doi.org/10.1016/J.ENVSOFT.2023.105658.

Fehn, N., Wall, W.A., Kronbichler, M., 2018. Robust and efficient discontinuous Galerkin methods for under-resolved turbulent incompressible flows. Journal of Computational Physics 372, 667–693. doi:http://dx.doi.org/10.1016/J.JCP.2018.06.037, arXiv:1801.08103.

Høye, T.T., Ärje, J., Bjerge, K., Hansen, O.L., Iosifidis, A., Leese, F., Mann, H.M., Meissner, K., Melvad, C., Raitoharju, J., 2021. Deep learning and computer vision will transform entomology. Proceedings of the National Academy of Sciences of the United States of America 118, e2002545117. URL: https://www.pnas.org/doi/abs/10.1073/pnas.2002545117, doi:http://dx.doi.org/10.1073/PNAS.2002545117/SUPPL_FILE/PNAS.2002545117.SAPP.PDF.

Karniadakis, G.E., Kevrekidis, I.G., Lu, L., Perdikaris, P., Wang, S., Yang, L., 2021. Physics-informed machine learning. Nature Reviews Physics 2021 3:6 3, 422–440. URL: https://www.nature.com/articles/s42254-021-00314-5, doi:http://dx.doi.org/10.1038/s42254-021-00314-5.

Knudde, N., Raes, W., De Bruycker, J., Dhaene, T., Stevens, N., 2020. Data-Efficient Gaussian Process Regression for Accurate Visible Light Positioning. IEEE Communications Letters 24, 1705–1709. doi:http://dx.doi.org/10.1109/LCOMM.2020.2990950.

Kochkov, D., Smith, J.A., Alieva, A., Wang, Q., Brenner, M.P., Hoyer, S., 2021. Machine learning–accelerated computational fluid dynamics. Proceedings of the National Academy of Sciences of the United States of America 118, e2101784118. URL: https://www.pnas.org/doi/abs/10.1073/pnas.2101784118, doi:http://dx.doi.org/10.1073/PNAS.2101784118/SUPPL_FILE/PNAS.2101784118.SAPP.PDF, arXiv:2102.01010.

Kumar, A., Ridha, S., Narahari, M., Ilyas, S.U., 2021. Physics-guided deep neural network to characterize non-Newtonian fluid flow for optimal use of energy resources. Expert Systems with Applications 183, 115409. doi:http://dx.doi.org/10.1016/J.ESWA.2021.115409.

Liu, P., Yuan, W., Fu, J., Jiang, Z., Hayashi, H., Neubig, G., 2023. Pre-train, Prompt, and Predict: A Systematic Survey of Prompting Methods in Natural Language Processing. ACM Computing Surveys 55. URL: https://dl.acm.org/doi/10.1145/3560815, doi:http://dx.doi.org/10.1145/3560815, arXiv:2107.13586.

Losada, I.J., Toimil, A., Muñoz, A., Garcia-Fletcher, A.P., Diaz-Simal, P., 2019. A planning strategy for the adaptation of coastal areas to climate change: The Spanish case. Ocean Coastal Management 182, 104983. doi:http://dx.doi.org/10.1016/J.OCECOAMAN.2019.104983.

Mahjoubi, S., Meng, W., Bao, Y., 2022. Logic-guided neural network for predicting steel-concrete interfacial behaviors. Expert Systems with Applications 198, 116820. doi:http://dx.doi.org/10.1016/J.ESWA.2022.116820.

Monaco, S., Apiletti, D., 2023. Training physics-informed neural networks: One learning to rule them all? Results in Engineering 18, 101023. doi:http://dx.doi.org/10.1016/J.RINENG.2023.101023.

Mukul, S.A., Alamgir, M., Sohel, M.S.I., Pert, P.L., Herbohn, J., Turton, S.M., Khan, M.S.I., Munim, S.A., Reza, A.H., Laurance, W.F., 2019. Combined effects of climate change and sea-level rise project dramatic habitat loss of the globally endangered Bengal tiger in the Bangladesh Sundarbans. Science of The Total Environment 663, 830–840. doi:http://dx.doi.org/10.1016/J.SCITOTENV.2019.01.383.

Partee, S., Ellis, M., Rigazzi, A., Shao, A.E., Bachman, S., Marques, G., Robbins, B., 2022. Using Machine Learning at scale in numerical simulations with SmartSim: An application to ocean climate modeling. Journal of Computational Science 62, 101707. doi:http://dx.doi.org/10.1016/J.JOCS.2022.101707, arXiv:2104.09355.

Pinto, G., Deltetto, D., Capozzoli, A., 2021. Data-driven district energy management with surrogate models and deep reinforcement learning. Applied Energy 304, 117642. doi:http://dx.doi.org/10.1016/J.APENERGY.2021.117642.

Raissi, M., Perdikaris, P., Karniadakis, G.E., 2019. Physics-informed neural networks: A deep learning framework for solving forward and inverse problems involving nonlinear partial differential equations. Journal of Computational Physics 378, 686–707. doi:http://dx.doi.org/10.1016/J.JCP.2018.10.045.

Ramachandran, P., Zoph, B., Le Google Brain, Q.V., 2017. Searching for Activation Functions. 6th International Conference on Learning Representations, ICLR 2018 - Workshop Track Proceedings URL: https://arxiv.

org/abs/1710.05941v2, doi:http://dx.doi.org/10.48550/arxiv.1710.05941, arXiv:1710.05941.

Sivarajah, U., Kamal, M.M., Irani, Z., Weerakkody, V., 2017. Critical analysis of Big Data challenges and analytical methods. Journal of Business Research 70, 263–286. doi:http://dx.doi.org/10.1016/J.JBUSRES.2016.08.001.

Vakili, S., Moss, H., Artemev, A., Dutordoir, V., Picheny, V., 2021. Scalable Thompson Sampling using Sparse Gaussian Process Models. Advances in Neural Information Processing Systems 34, 5631–5643.

Wang, K.A., Pleiss, G., Gardner, J.R., Tyree, S., Weinberger, K.Q., Wilson, A.G., 2019. Exact Gaussian Processes on a Million Data Points. Advances in Neural Information Processing Systems 32.

Wang, S., Sankaran, S., Perdikaris, P., 2022. RESPECTING CAUSALITY IS ALL YOU NEED FOR TRAINING PHYSICS-INFORMED NEURAL NETWORKS URL: https://arxiv.org/abs/2203.07404, arXiv:2203.07404.

Weber, T., Corotan, A., Hutchinson, B., Kravitz, B., Link, R., 2020. Technical note: Deep learning for creating surrogate models of precipitation in earth system models. Atmospheric Chemistry and Physics 20, 2303–2317. URL: https://acp.copernicus.org/articles/20/2303/2020/, doi:http://dx.doi.org/10.5194/acp-20-2303-2020.

Weinberg, K., Wieners, C., 2021. Dynamic phase-field fracture with a first-order discontinuous Galerkin method for elastic waves. Computer Methods in Applied Mechanics and Engineering 389. URL: http://arxiv.org/abs/2106.15193http://dx.doi.org/10.1016/j.cma.2021.114330, doi:http://dx.doi.org/10.1016/j.cma.2021.114330, arXiv:2106.15193v2.